Crack Analysis in Magneto-Electro-Elastic Solids

Jan Sladek[1, a], Vladimir Sladek[1,b] and Peter Solek[2,c]

[1]Institute of Construction and Architecture, Slovak Academy of Sciences, 84503 Bratislava, Slovakia

[2]Department of Mechanics, Slovak Technical University, Bratislava, Slovakia

[a]sladek@savba.sk, [b]vladimir.sladek@savba.sk, [c]peter.solek@stuba.sk

Keywords: Meshless local Petrov-Galerkin method (MLPG), Moving least-squares (MLS) interpolation, cracks, intensity factors, 2-D dynamic problems

Abstract. A meshless method based on the local Petrov-Galerkin approach is proposed for crack analysis in two-dimensional (2-D) magneto-electric-elastic solids with continuously varying material properties. Stationary and transient dynamic problems are considered in this paper. The local weak formulation is employed on circular subdomains where surrounding nodes randomly spread over the analyzed domain. The test functions are taken as unit step functions in derivation of the local integral equations (LIEs). The moving least-squares (MLS) method is adopted for the approximation of the physical quantities in the LIEs.

Introduction

Modern smart structures made of piezoelectric and piezomagnetic materials offer certain potential performance advantages over conventional ones due to their capability of converting the energy from one type to other (among magnetic, electric, and mechanical) [1]. Former activities were focused on modeling of magneto-electric-elastic fields to determine the field variables [2,3]. Recently, increasing interest is devoted to fracture mechanics of magneto-electric-elastic materials [4-8]. All above mentioned works are made under a static deformation assumption. However, dynamic fracture analyses are occurring in literature very seldom. Some works on relatively simple anti-plane problems have been published [9,10].

Magnetoelectric coupling plays an important role in the dynamic behaviour of certain materials, especially compounds which possess simultaneously ferroelectric and ferromagnetic phases. Remarkably large magnetoelectric effects are observed in composites rather than in either single phase/constituent [11]. If the volume fraction of constituents is varying in a predominant direction we are talking about functionally graded materials (FGMs). A review on various aspects of FGMs can be found in the monograph of Suresh and Mortensen [12]. According the best of authors' knowledge there is available only one paper [13] with applications to continuously nonhomogeneous magneto-electric materials.

The solution of general boundary value problems for continuously nonhomogeneous magneto-electric-elastic solids requires advanced numerical methods due to the high mathematical complexity. Besides this complication, the magnetic, electric and mechanical fields are coupled with each other in the constitutive equations. In spite of the great success of the finite element method (FEM) and boundary element method (BEM) as effective numerical tools for the solution of boundary value problems in magneto-electric-elastic solids, there is still a growing interest in the development of new advanced numerical methods. In recent years, meshless formulations are becoming popular due to their high adaptability and low costs to prepare input and output data in numerical analysis. A variety of meshless methods has been proposed so far with some of them applied only to piezoelectric problems [14,15]. The meshless local Petrov-Galerkin (MLPG) method is a fundamental base for the derivation of many meshless formulations, since trial and test functions can be chosen from different functional spaces. Recently, the MLPG method with a Heaviside step function as the test functions [16,17] has been applied to solve two-dimensional (2-D) homogeneous piezoelectric problems [18]. In the present paper, the MLPG method is extended to 2-D continuously nonhomogeneous magneto-electric-elastic solids with cracks. The coupled governing partial differential equations are satisfied in a weak form on small fictitious subdomains. Nodal points are introduced and spread on the analyzed domain and each node is surrounded by a small circle for simplicity, but without loss of generality. The spatial variations of the displacements and the electric potential are approximated by the moving least-squares scheme [16]. After performing the spatial integrations, a system of linear algebraic equations for the unknown nodal values is obtained.

Local integral equations

Basic equations of phenomenological theory of nonconducting elastic materials consist of the governing equations (Maxwell's equations, the balance of momentum) and the constitutive relationships. The governing equations completed by the boundary and initial conditions should be solved for unknown primary field variables such as the elastic displacement vector field $u_i(\mathbf{x},\tau)$, the electric potential $\psi(\mathbf{x},\tau)$ (or its gradient called the electric vector field $E_i(\mathbf{x},\tau)$), and the magnetic potential $\mu(\mathbf{x},\tau)$ (or its gradient called the magnetic intensity field $H_i(\mathbf{x},\tau)$). The constitutive equations co-relate the primary fields $\{u_i, E_i, H_i\}$ with the secondary fields $\{\sigma_{ij}, D_i, B_i\}$ which are the stress tensor field, the electric displacement vector field, and the magnetic induction vector field, respectively.
The electromagnetic fields can be considered like quasi-static [19]. Then, the Maxwell equations are reduced to two scalar equations

$$D_{j,j}(\mathbf{x},\tau)=0, \tag{1}$$

$$B_{j,j}(\mathbf{x},\tau)=0, \tag{2}$$

The rest vector Maxwell's equations in quasi-static approximation, $\nabla\times\mathbf{E}=0$ and $\nabla\times\mathbf{H}=0$, are satisfied identically by appropriate representation of the fields $\mathbf{E}(\mathbf{x},\tau)$ and $\mathbf{H}(\mathbf{x},\tau)$ as gradients of scalar electric and magnetic potentials $\psi(\mathbf{x},\tau)$ and $\mu(\mathbf{x},\tau)$, respectively,

$$E_j(\mathbf{x},\tau)=-\psi_{,j}(\mathbf{x},\tau)\ , \tag{3}$$

$$H_j(\mathbf{x},\tau)=-\mu_{,j}(\mathbf{x},\tau)\ . \tag{4}$$

To complete the set of governing equations, eqs. (1) and (2) need to be supplied by the equation of motion in elastic continuum

$$\sigma_{ij,j}(\mathbf{x},\tau)+X_i(\mathbf{x},\tau)=\rho\ddot{u}_i(\mathbf{x},\tau), \tag{5}$$

where $\ddot{u}_i$, ρ and X_i denote the acceleration of displacements, the mass density, and the body force vector, respectively. A comma after a quantity represents the partial derivatives of the quantity and a dot is used for the time derivative.

The constitutive equations involving the general electro-magneto-elastic interaction [11] to media with spatially dependent material coefficients for continuously non-homogeneous media are given

$$\sigma_{ij}(\mathbf{x},\tau)=c_{ijkl}(\mathbf{x})\varepsilon_{kl}(\mathbf{x},\tau)-e_{kij}(\mathbf{x})E_k(\mathbf{x},\tau)-d_{kij}(\mathbf{x})H_k(\mathbf{x},\tau), \tag{6}$$

$$D_j(\mathbf{x},\tau)=e_{jkl}(\mathbf{x})\varepsilon_{kl}(\mathbf{x},\tau)+h_{jk}(\mathbf{x})E_k(\mathbf{x},\tau)+\alpha_{jk}(\mathbf{x})H_k(\mathbf{x},\tau), \tag{7}$$

$$B_j(\mathbf{x},\tau)=d_{jkl}(\mathbf{x})\varepsilon_{kl}(\mathbf{x},\tau)+\alpha_{kj}(\mathbf{x})E_k(\mathbf{x},\tau)+\gamma_{jk}(\mathbf{x})H_k(\mathbf{x},\tau), \tag{8}$$

where ε_{ij} is the strain tensor and $c_{ijkl}(\mathbf{x})$, $h_{jk}(\mathbf{x})$, and $\gamma_{jk}(\mathbf{x})$ are the elastic coefficients, dielectric permittivities, and magnetic permeabilities, respectively; $e_{kij}(\mathbf{x})$, $d_{kij}(\mathbf{x})$, and $\alpha_{jk}(\mathbf{x})$ are the piezoelectric, piezomagnetic, and magnetoelectric coefficients, respectively. Owing to transient loadings, inertial effects and coupling, the elastic fields as well as electromagnetic fields are time dependent, though the fields E_i and H_i are treated in quasi-static approximation.

In case of some crystal symmetries, one can formulate also the plane-deformation problems [19]. For instance, in the crystals of hexagonal symmetry (class $6mm$) with x_3 being the 6-order symmetry axis and assuming $u_2 = 0$ as well as the independence on x_2, i.e. $(\bullet)_{,2} = 0$, we have $\varepsilon_{22} = \varepsilon_{23} = \varepsilon_{12} = E_2 = H_2 = 0$. Then, the constitutive equations (6) - (8) are reduced to the following form

$$\begin{bmatrix} \sigma_{11} \\ \sigma_{33} \\ \sigma_{13} \end{bmatrix} = \begin{bmatrix} c_{11} & c_{13} & 0 \\ c_{13} & c_{33} & 0 \\ 0 & 0 & c_{44} \end{bmatrix} \begin{bmatrix} \varepsilon_{11} \\ \varepsilon_{33} \\ 2\varepsilon_{13} \end{bmatrix} - \begin{bmatrix} 0 & e_{31} \\ 0 & e_{33} \\ e_{15} & 0 \end{bmatrix} \begin{bmatrix} E_1 \\ E_3 \end{bmatrix} - \begin{bmatrix} 0 & d_{31} \\ 0 & d_{33} \\ d_{15} & 0 \end{bmatrix} \begin{bmatrix} H_1 \\ H_3 \end{bmatrix} =$$

$$= \mathbf{C}(\mathbf{x}) \begin{bmatrix} \varepsilon_{11} \\ \varepsilon_{33} \\ 2\varepsilon_{13} \end{bmatrix} - \mathbf{L}(\mathbf{x}) \begin{bmatrix} E_1 \\ E_3 \end{bmatrix} - \mathbf{K}(\mathbf{x}) \begin{bmatrix} H_1 \\ H_3 \end{bmatrix}, \qquad (9)$$

$$\begin{bmatrix} D_1 \\ D_3 \end{bmatrix} = \begin{bmatrix} 0 & 0 & e_{15} \\ e_{31} & e_{33} & 0 \end{bmatrix} \begin{bmatrix} \varepsilon_{11} \\ \varepsilon_{33} \\ 2\varepsilon_{13} \end{bmatrix} + \begin{bmatrix} h_{11} & 0 \\ 0 & h_{33} \end{bmatrix} \begin{bmatrix} E_1 \\ E_3 \end{bmatrix} + \begin{bmatrix} \alpha_{11} & 0 \\ 0 & \alpha_{33} \end{bmatrix} \begin{bmatrix} H_1 \\ H_3 \end{bmatrix} =$$

$$= \mathbf{G}(\mathbf{x}) \begin{bmatrix} \varepsilon_{11} \\ \varepsilon_{33} \\ 2\varepsilon_{13} \end{bmatrix} + \mathbf{H}(\mathbf{x}) \begin{bmatrix} E_1 \\ E_3 \end{bmatrix} + \mathbf{A}(\mathbf{x}) \begin{bmatrix} H_1 \\ H_3 \end{bmatrix}, \qquad (10)$$

$$\begin{bmatrix} B_1 \\ B_3 \end{bmatrix} = \begin{bmatrix} 0 & 0 & d_{15} \\ d_{31} & d_{33} & 0 \end{bmatrix} \begin{bmatrix} \varepsilon_{11} \\ \varepsilon_{33} \\ 2\varepsilon_{13} \end{bmatrix} + \begin{bmatrix} \alpha_{11} & 0 \\ 0 & \alpha_{33} \end{bmatrix} \begin{bmatrix} E_1 \\ E_3 \end{bmatrix} + \begin{bmatrix} \gamma_{11} & 0 \\ 0 & \gamma_{33} \end{bmatrix} \begin{bmatrix} H_1 \\ H_3 \end{bmatrix} =$$

$$= \mathbf{R}(\mathbf{x}) \begin{bmatrix} \varepsilon_{11} \\ \varepsilon_{33} \\ 2\varepsilon_{13} \end{bmatrix} + \mathbf{A}(\mathbf{x}) \begin{bmatrix} E_1 \\ E_3 \end{bmatrix} + \mathbf{M}(\mathbf{x}) \begin{bmatrix} H_1 \\ H_3 \end{bmatrix}, \qquad (11)$$

The following essential and natural boundary conditions are assumed for the mechanical field

$$u_i(\mathbf{x},\tau) = \tilde{u}_i(\mathbf{x},\tau), \quad \text{on} \quad \Gamma_u,$$

$$t_i(\mathbf{x},\tau) = \sigma_{ij} n_j = \tilde{t}_i(\mathbf{x},\tau), \quad \text{on} \quad \Gamma_t, \quad \Gamma = \Gamma_u \cup \Gamma_t.$$

For the electrical field, we assume

$$\psi(\mathbf{x},\tau) = \tilde{\psi}(\mathbf{x},\tau), \quad \text{on} \quad \Gamma_p,$$

$$n_i(\mathbf{x}) D_i(\mathbf{x},\tau) \equiv Q(\mathbf{x},\tau) = \tilde{Q}(\mathbf{x},\tau), \quad \text{on} \quad \Gamma_q, \quad \Gamma = \Gamma_p \cup \Gamma_q$$

and for the magnetic field

$$\mu(\mathbf{x},\tau) = \tilde{\mu}(\mathbf{x},\tau), \quad \text{on} \quad \Gamma_a,$$

$$n_i(\mathbf{x}) B_i(\mathbf{x},\tau) \equiv S(\mathbf{x},\tau) = \tilde{S}(\mathbf{x},\tau), \quad \text{on} \quad \Gamma_b, \quad \Gamma = \Gamma_a \cup \Gamma_b$$

where Γ_u is the part of the global boundary Γ with prescribed displacements, while on Γ_t, Γ_p, Γ_q, Γ_a, and Γ_b the traction vector, the electric potential, the normal component of the electric displacement vector, the magnetic potential and the magnetic flux are prescribed, respectively.

Recall that $\tilde{Q}(\mathbf{x},\tau)$ can be considered approximately as the surface density of free charge, provided that the permittivity of the solid is much greater than that of the surrounding medium (vacuum).

Applying the Laplace-transform to the governing equations (5) one obtains

$$\bar{\sigma}_{ij,j}(\mathbf{x},p)-\rho(\mathbf{x})p^2\bar{u}_i(\mathbf{x},p)=-\bar{F}_i(\mathbf{x},p)\,, \tag{12}$$

where

$$\bar{F}_i(\mathbf{x},p)=\bar{X}_i(\mathbf{x},p)+pu_i(\mathbf{x},0)+\dot{u}_i(\mathbf{x},0)\,,$$

is the re-defined body force in the Laplace-transformed domain with the initial boundary conditions for the displacements and velocities $\dot{u}_i(\mathbf{x},0)$. Recall that the subscripts take now values $i\in\{1,3\}$.

The MLPG method constructs a weak-form over the local fictitious subdomains such as Ω_s, which is a small region constructed for each node inside the global domain [16]. The local subdomains overlap each other, and cover the whole global domain Ω. The local subdomains could be of any geometrical shape and size. In the present paper, the local subdomains are taken to be of a circular shape for simplicity. The local weak-form of the governing equation (12) can be written as

$$\int_{\Omega_s}\left[\bar{\sigma}_{ij,j}(\mathbf{x},p)-\rho(\mathbf{x})p^2\bar{u}_i(\mathbf{x},p)+\bar{F}_i(\mathbf{x},p)\right]u_{ik}^*(\mathbf{x})\,d\Omega\;=0\,, \tag{13}$$

where $u_{ik}^*(\mathbf{x})$ is a test function.

Applying the Gauss divergence theorem to eq. (13) one obtains

$$\int_{\partial\Omega_s}\bar{\sigma}_{ij}(\mathbf{x},p)n_j(\mathbf{x})u_{ik}^*(\mathbf{x})d\Gamma-\int_{\Omega_s}\bar{\sigma}_{ij}(\mathbf{x},p)u_{ik,j}^*(\mathbf{x})d\Omega+\int_{\Omega_s}\left[\bar{F}_i(\mathbf{x},p)-\rho(\mathbf{x})p^2\bar{u}_i(\mathbf{x},p)\right]u_{ik}^*(\mathbf{x})d\Omega=0\,, \tag{14}$$

where $\partial\Omega_s$ is the boundary of the local subdomain which consists of three parts $\partial\Omega_s=L_s\cup\Gamma_{st}\cup\Gamma_{su}$ [16]. Here, L_s is the local boundary that is totally inside the global domain, Γ_{st} is the part of the local boundary which coincides with the global traction boundary, i.e., $\Gamma_{st}=\partial\Omega_s\cap\Gamma_t$, and similarly Γ_{su} is the part of the local boundary that coincides with the global displacement boundary, i.e., $\Gamma_{su}=\partial\Omega_s\cap\Gamma_u$.

By choosing a Heaviside step function as the test function $u_{ik}^*(\mathbf{x})$ in each subdomain, the local weak-form (14) is converted into the following local boundary-domain integral equations

$$\int_{L_s+\Gamma_{su}}\bar{t}_i(\mathbf{x},p)d\Gamma-\int_{\Omega_s}\rho(\mathbf{x})p^2\bar{u}_i(\mathbf{x},p)d\Omega=-\int_{\Gamma_{st}}\tilde{\bar{t}}_i(\mathbf{x},p)d\Gamma-\int_{\Omega_s}\bar{F}_i(\mathbf{x},p)d\Omega\,. \tag{15}$$

Similarly, the local weak-form of the governing equation (2) can be written as

$$\int_{\Omega_s}\bar{D}_{j,j}(\mathbf{x},p)v^*(\mathbf{x})\,d\Omega\;=0\,, \tag{16}$$

where $v^*(\mathbf{x})$ is a test function.

Applying the Gauss divergence theorem to the local weak-form (16) and choosing the Heaviside step function as the test function $v^*(\mathbf{x})$ one can obtain

$$\int_{L_s+\Gamma_{sp}}\bar{Q}(\mathbf{x},p)d\Gamma=-\int_{\Gamma_{sq}}\tilde{\bar{Q}}(\mathbf{x},p)d\Gamma\,, \tag{17}$$

where

$$\bar{Q}(\mathbf{x},p)=\bar{D}_j(\mathbf{x},p)n_j(\mathbf{x})=\left[e_{jkl}\bar{u}_{k,l}(\mathbf{x},p)-h_{jk}\bar{\psi}_{,k}(\mathbf{x},p)-\alpha_{jk}\bar{\mu}_{,k}(\mathbf{x},p)\right]n_j\,.$$

The local integral equation corresponding to the third governing equation (3) has the form

$$\int_{L_s+\Gamma_{sa}}\bar{S}(\mathbf{x},p)d\Gamma=-\int_{\Gamma_{sb}}\tilde{\bar{S}}(\mathbf{x},p)d\Gamma\,, \tag{18}$$

where magnetic flux is given by
$\bar{S}(\mathbf{x},p)=\bar{B}_j(\mathbf{x},p)n_j(\mathbf{x})=\left[d_{jkl}\bar{u}_{k,l}(\mathbf{x},p)-\alpha_{kj}\psi_{,k}(\mathbf{x},p)-\gamma_{jk}\mu_{,k}(\mathbf{x},p)\right]n_j$.

The trial functions are chosen to be the MLS approximations by using a number of nodes spreading over the domain of influence. According to the MLS method [16], the approximation of the displacement can be given as

$$\mathbf{u}^h(\mathbf{x})=\sum_{i=1}^{m}p_i(\mathbf{x})a_i(\mathbf{x})=\mathbf{p}^T(\mathbf{x})\mathbf{a}(\mathbf{x}),$$

where $\mathbf{p}^T(\mathbf{x})=\{p_1(\mathbf{x}),p_2(\mathbf{x}),...p_m(\mathbf{x})\}$ is a vector of complete basis functions of order m and $\mathbf{a}(\mathbf{x})=\{a_1(\mathbf{x}),a_2(\mathbf{x}),...a_m(\mathbf{x})\}$ is a vector of unknown parameters that depend on **x**. The basis functions are not required to be polynomials. It is convenient to introduce $r^{-1/2}$ singularity for secondary fields at the crack tip vicinity for modelling of fracture problems. Then, the basis functions can be considered in the following form

$$\mathbf{p}^T(\mathbf{x})=\left\{1,x_1,x_2,\sqrt{r}\cos(\theta/2),\sqrt{r}\sin(\theta/2),\sqrt{r}\sin(\theta/2)\sin\theta,\sqrt{r}\cos(\theta/2)\sin\theta\right\}\quad \text{for m=7}$$

where r and θ are polar coordinates with the crack tip as the origin.

The approximated functions for the Laplace transforms of the mechanical displacements, the electric and magnetic potentials can be written as

$$\bar{\mathbf{u}}^h(\mathbf{x},p)=\mathbf{\Phi}^T(\mathbf{x})\cdot\hat{\mathbf{u}}=\sum_{a=1}^{n}\phi^a(\mathbf{x})\hat{\mathbf{u}}^a(p),\qquad \bar{\psi}^h(\mathbf{x},p)=\sum_{a=1}^{n}\phi^a(\mathbf{x})\hat{\psi}^a(p),$$

$$\bar{\mu}^h(\mathbf{x},p)=\sum_{a=1}^{n}\phi^a(\mathbf{x})\hat{\mu}^a(p), \tag{19}$$

where the nodal values $\hat{\mathbf{u}}^a(p)=\left(\hat{u}_1^a(p),\,\hat{u}_3^a(p)\right)^T$, $\hat{\psi}^a(p)$ and $\hat{\mu}^a(p)$ are fictitious parameters for the displacements, the electric and magnetic potentials, respectively, and $\phi^a(\mathbf{x})$ is the shape function associated with the node a.

The Laplace transform of traction vectors $\bar{t}_i(\mathbf{x},p)$ at a boundary point $\mathbf{x}\in\partial\Omega_s$ are approximated in terms of the same nodal values $\hat{\mathbf{u}}^a(p)$ as

$$\bar{\mathbf{t}}^h(\mathbf{x},p)=\mathbf{N}(\mathbf{x})\mathbf{C}(\mathbf{x})\sum_{a=1}^{n}\mathbf{B}^a(\mathbf{x})\hat{\mathbf{u}}^a(p)+\mathbf{N}(\mathbf{x})\mathbf{L}(\mathbf{x})\sum_{a=1}^{n}\mathbf{P}^a(\mathbf{x})\hat{\psi}^a(p)+\mathbf{N}(\mathbf{x})\mathbf{K}(\mathbf{x})\sum_{a=1}^{n}\mathbf{P}^a(\mathbf{x})\hat{\mu}^a(p), \tag{20}$$

where the matrices $\mathbf{C}(\mathbf{x})$, $\mathbf{L}(\mathbf{x})$, and $\mathbf{K}(\mathbf{x})$ are defined in eq. (9), the matrix **N(x)** is related to the normal vector **n(x)** on $\partial\Omega_s$ by

$$\mathbf{N}(\mathbf{x})=\begin{bmatrix} n_1 & 0 & n_3 \\ 0 & n_3 & n_1 \end{bmatrix}$$

and finally, the matrices $\mathbf{B}^a$ and $\mathbf{P}^a$ are represented by the gradients of the shape functions as

$$\mathbf{B}^a(\mathbf{x})=\begin{bmatrix} \phi_{,1}^a & 0 \\ 0 & \phi_{,3}^a \\ \phi_{,3}^a & \phi_{,1}^a \end{bmatrix},\qquad \mathbf{P}^a(\mathbf{x})=\begin{bmatrix} \phi_{,1}^a \\ \phi_{,3}^a \end{bmatrix}.$$

Similarly the Laplace-transform of the normal component of the electric displacement vector $\bar{Q}(\mathbf{x},p)$ can be approximated by

$$\bar{Q}^h(\mathbf{x},p)=\mathbf{N}_1(\mathbf{x})\mathbf{G}(\mathbf{x})\sum_{a=1}^{n}\mathbf{B}^a(\mathbf{x})\hat{\mathbf{u}}^a(p)-\mathbf{N}_1(\mathbf{x})\mathbf{H}(\mathbf{x})\sum_{a=1}^{n}\mathbf{P}^a(\mathbf{x})\hat{\psi}^a(p)-\mathbf{N}_1(\mathbf{x})\mathbf{A}(\mathbf{x})\sum_{a=1}^{n}\mathbf{P}^a(\mathbf{x})\hat{\mu}^a(p), \tag{21}$$

where the matrices $\mathbf{G}(\mathbf{x})$, $\mathbf{H}(\mathbf{x})$, and $\mathbf{A}(\mathbf{x})$ are defined in eq. (10) and

$\mathbf{N}_1(\mathbf{x}) = [n_1 \quad n_3]$.

Eventually, the Laplace-transform of the magnetic flux $\bar{S}(\mathbf{x}, p)$ is approximated by

$$\bar{S}^h(\mathbf{x}, p) = \mathbf{N}_1(\mathbf{x})\mathbf{R}(\mathbf{x})\sum_{a=1}^{n}\mathbf{B}^a(\mathbf{x})\hat{\mathbf{u}}^a(p) - \mathbf{N}_1(\mathbf{x})\mathbf{A}(\mathbf{x})\sum_{a=1}^{n}\mathbf{P}^a(\mathbf{x})\hat{\psi}^a(p) - \mathbf{N}_1(\mathbf{x})\mathbf{M}(\mathbf{x})\sum_{a=1}^{n}\mathbf{P}^a(\mathbf{x})\hat{\mu}^a(p), \quad (22)$$

with the matrices $\mathbf{R}(\mathbf{x})$ and $\mathbf{M}(\mathbf{x})$ being defined in eq. (11).

Furthermore, in view of the MLS-approximation (20) - (22) for the unknown quantities in the local boundary-domain integral equations (15), (17) and (18), we obtain their discretized forms as

$$\sum_{a=1}^{n}\left(\int_{L_s+\Gamma_{st}} \mathbf{N}(\mathbf{x})\mathbf{C}(\mathbf{x})\mathbf{B}^a(\mathbf{x})d\Gamma - \mathbf{I}\rho p^2 \int_{\Omega_s}\phi^a(\mathbf{x})d\Omega\right)\hat{\mathbf{u}}^a(p) + \sum_{a=1}^{n}\left(\int_{L_s+\Gamma_{sq}} \mathbf{N}(\mathbf{x})\mathbf{L}(\mathbf{x})\mathbf{P}^a(\mathbf{x})d\Gamma\right)\hat{\boldsymbol{\psi}}^a(p) +$$

$$+\sum_{a=1}^{n}\left(\int_{L_s+\Gamma_{sb}} \mathbf{N}(\mathbf{x})\mathbf{K}(\mathbf{x})\mathbf{P}^a(\mathbf{x})d\Gamma\right)\hat{\boldsymbol{\mu}}^a(p) = -\int_{\Gamma_{st}}\tilde{\bar{\mathbf{t}}}(\mathbf{x}, p)d\Gamma - \int_{\Omega_s}\bar{\mathbf{F}}(\mathbf{x}, p)d\Omega\ , \quad (23)$$

$$\sum_{a=1}^{n}\left(\int_{L_s+\Gamma_{sp}} \mathbf{N}_1(\mathbf{x})\mathbf{G}(\mathbf{x})\mathbf{B}^a(\mathbf{x})d\Gamma\right)\hat{\mathbf{u}}^a(p) - \sum_{a=1}^{n}\left(\int_{L_s+\Gamma_{sp}} \mathbf{N}_1(\mathbf{x})\mathbf{H}(\mathbf{x})\mathbf{P}^a(\mathbf{x})d\Gamma\right)\hat{\boldsymbol{\psi}}^a(p) -$$

$$-\sum_{a=1}^{n}\left(\int_{L_s+\Gamma_{sp}} \mathbf{N}_1(\mathbf{x})\mathbf{A}(\mathbf{x})\mathbf{P}^a(\mathbf{x})d\Gamma\right)\hat{\boldsymbol{\mu}}^a(p) = -\int_{\Gamma_{sq}}\tilde{\bar{Q}}(\mathbf{x}, p)d\Gamma\,, \quad (24)$$

$$\sum_{a=1}^{n}\left(\int_{L_s+\Gamma_{sp}} \mathbf{N}_1(\mathbf{x})\mathbf{R}(\mathbf{x})\mathbf{B}^a(\mathbf{x})d\Gamma\right)\hat{\mathbf{u}}^a(p) - \sum_{a=1}^{n}\left(\int_{L_s+\Gamma_{sp}} \mathbf{N}_1(\mathbf{x})\mathbf{A}(\mathbf{x})\mathbf{P}^a(\mathbf{x})d\Gamma\right)\hat{\boldsymbol{\psi}}^a(p) -$$

$$-\sum_{a=1}^{n}\left(\int_{L_s+\Gamma_{sp}} \mathbf{N}_1(\mathbf{x})\mathbf{M}(\mathbf{x})\mathbf{P}^a(\mathbf{x})d\Gamma\right)\hat{\boldsymbol{\mu}}^a(p) = -\int_{\Gamma_{sq}}\tilde{\bar{S}}(\mathbf{x}, p)d\Gamma\,, \quad (25)$$

which are considered on the sub-domains adjacent to the interior nodes as well as to the boundary nodes on Γ_{st}, Γ_{sq} and Γ_{sb}. In equation (23), $\mathbf{I}$ is a unit matrix.

Collecting the discretized local boundary-domain integral equations together with the discretized boundary conditions for the displacements, the electrical and magnetic potentials results in the complete system of linear algebraic equations for the computation of the nodal unknowns.

Numerical examples

An edge crack in a finite magneto-electric-elastic strip is analyzed. The geometry of the strip is given in Fig. 1 with the following values are selected: $a = 0.5$, $a/w = 0.4$ and $h/w = 1.2$. Due to the symmetry of the problem with respect to the x_1-axis, only a half of the strip is modeled. We have used again 930 equidistantly distributed nodes for the MLS approximation of the physical fields. The functionally graded material properties in the x_1-direction are considered

$$f_{ij}(\mathbf{x}) = f_{ij0}\exp(\gamma_f x_1)\,, \quad (26)$$

where the symbol f_{ij} is commonly used for partial material coefficients and f_{ij0} correspond to the material parameters of $BaTiO_3$-$CoFe_2O_4$ composite given by Li [20]. We have considered the same exponential gradient for all coefficients with value $\gamma = 2$ in the numerical calculations. The strip is subjected to an impact mechanical load with Heaviside time variation and the intensity $\sigma_0 = 1Pa$.

The impermeable boundary conditions for the electric displacement and magnetic flux on crack surfaces are considered.

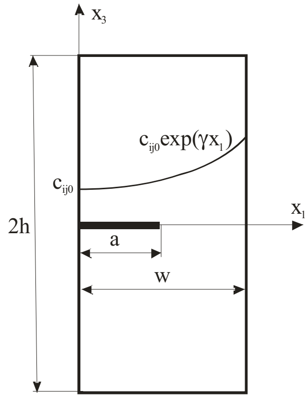

Fig. 1 An edge crack in a finite strip with graded material properties in x_1-direction

In the crack tip vicinity, the displacements and potentials show the classical $\sqrt{r}$ asymptotic behaviour. Hence, correspondingly, stresses, the electrical displacement and magnetic induction exhibit $1/\sqrt{r}$ behaviour, where r is the radial polar coordinate with origin at the crack tip. Garcia-Sanchez et al. [21] extended the approach used in piezoelectricity to magnetoelectroelasticity to obtain asymptotic expression of generalized intensity factors.

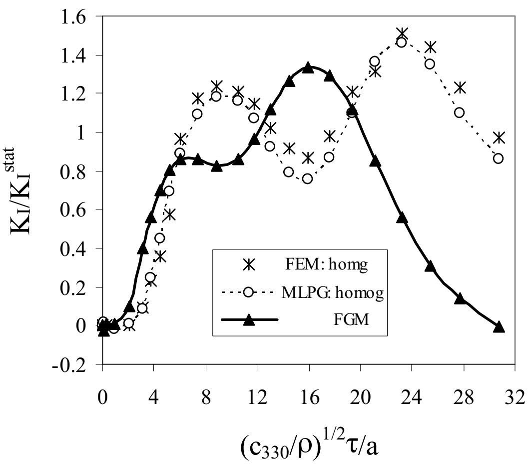

Fig. 2 Normalized SIF for an edge crack in a strip under a pure mechanical load $\sigma_0 H(\tau - 0)$

The time variation of the normalized stress intensity factor is given in Fig. 2, where $K_I^{stat} = 2.642\text{Pa}\cdot\text{m}^{1/2}$ .For a mechanical FGMs along the x_1 -coordinate and a uniform mass density, the wave propagation is growing with x_1 . Therefore, the peak value of the SIF is reached in a shorter time instant in functionally graded strip than in a homogeneous one. The maximum value of the SIF is only slightly reduced for the FGM cracked strip.

Summary

A meshless local Petrov-Galerkin method (MLPG) is presented for 2-D crack problems in continuously nonhomogeneous and linear magneto-electric-elastic solids. The analyzed domain is divided into small overlapping circular subdomains. A unit step function is used as the test function in the local weak-form of the governing partial differential equations. The moving least-squares (MLS) scheme is adopted for the approximation of the physical field quantities. The present method provides an alternative numerical tool to many existing computational methods like the FEM or BEM. The main advantage of the present method is its simplicity. Compared to the conventional BEM, the present method requires no fundamental solutions and all integrands in the present formulation are regular. Thus, no special numerical techniques are required to evaluate the integrals. It should be noted here that the fundamental solutions are not available for magneto-electric-elastic solids with continuously varying material properties in general cases. The present formulation also possesses the generality of the FEM. Therefore, the method is promising for numerical analysis of multi-field problems.

References

[1] M. Avellaneda and G. Harshe: J. Intell. Mater. Sys. Struct. Vol. 5 (1994), p. 501.

[2] V.I. Alshits, A.N. Darinski and J. Lothe: Wave Motion Vol. 16 (1992), p. 265.

[3] E. Pan: ASME J. Appl. Mech. Vol. 68 (2001), p. 608.

[4] C.F. Gao, H. Kessler and H. Balke: Int. J. Engn. Sci. Vol. 41 (2003), p. 969.

[5] Z.F. Song and G.C. Sih: Theor. Appl. Fract. Mech. Vol. 39 (2003), p. 189.

[6] W.Y. Tian and U. Gabbert: Mech. Mater. Vol. 37 (2005), p. 565.

[7] K.Q. Hu and Z. Zhong: Mech. Res. Comm. Vol. 33 (2006), p. 482.

[8] B.L. Wang and Y.W. Mai: Int. J. Solids Struct. Vol. 44 (2007), p. 387.

[9] J.K. Du, Y.P. Shen, D.Y. Ye and F.R. Yue: Int. J. Engn. Sci. Vol. 42 (2004), p. 887.

[10] R.K.L. Su and W.J. Feng: Computer& Structures Vol. 78 (2007), p. 119.

[11] C.W. Nan: Phys. Rev. B Vol. 50 (1994), p. 6082.

[12] S. Suresh and A. Mortensen: *Fundamentals of Functionally Graded Materials* (Institute of Materials, London 1998).

[13] W.J. Feng and R.K.L. Su: Int. J. Solids Struct. Vol. 43 (2006), p. 5196.

[14] R.R. Ohs and N.R. Aluru: Comput. Mech. Vol. 27 (2001), p. 23.

[15] G.R. Liu, K.Y. Dai, K.M. Lim and Y.T. Gu: Comput. Mech. Vol. 29 (2002), p. 510.

[16] S.N. Atluri: *The Meshless Method, (MLPG) For Domain & BIE Discretizations* (Tech Science Press, Forsyth 2004).

[17] J. Sladek, V. Sladek and S.N. Atluri: CMES: Comp. Mod. Engn. & Sci. Vol. 6 (2004), p. 477.

[18] J. Sladek, V. Sladek, Ch. Zhang, P. Solek and E. Pan: Int. J. Fracture Vol. 145 (2007), p. 313.

[19] V.Z. Parton and B.A. Kudryavtsev: *Electromagnetoelasticity, Piezoelectrics and Electrically Conductive Solids* (Gordon and Breach Science Publishers, New York 1988).

[20] J.Y. Li: Int. J. Engn. Sci. Vol. 38 (2000), p. 1993.

[21] F. Garcia-Sanchez, R. Rojas-Diaz, A. Saez and Ch. Zhang: Theor. Appl. Fract. Mech. Vol. 47 (2007), p. 192.